

Pulmonary toxicity of well-dispersed multi-wall carbon nanotubes following inhalation and intratracheal instillation

Yasuo Morimoto¹, Masami Hirohashi¹, Akira Ogami¹, Takako Oyabu¹, Toshihiko Myojo¹, Motoi Todoroki¹, Makoto Yamamoto¹, Masayoshi Hashiba¹, Yohei Mizuguchi¹, Byeong Woo Lee¹, Etsushi Kuroda², Manabu Shimada³, Wei-Ning Wang³, Kazuhiro Yamamoto⁴, Katsuhide Fujita⁴, Shigehisa Endoh⁴, Kunio Uchida⁴, Norihiro Kobayashi⁴, Kohei Mizuno⁴, Masaharu Inada⁴, Hiroaki Tao⁴, Tetsuya Nakazato⁴, Junko Nakanishi⁴ & Isamu Tanaka¹

¹Institute of Industrial Ecological Sciences, ²Department of Immunology and Parasitology, School of Medicine, both at University of Occupational and Environmental Health, Japan, Kitakyushu, ³Hiroshima University, Hiroshima and ⁴National Institute of Advanced Industrial Science and Technology, Tsukuba, Japan

Abstract

Multi-walled carbon nanotubes (MWCNTs), dispersed in suspensions consisting mainly of individual tubes, were used for intratracheal instillation and inhalation studies. Rats intratracheally received a dose of 0.2 mg, or 1 mg of MWCNTs and were sacrificed from 3 days to 6 months. MWCNTs induced a pulmonary inflammation, as evidenced by a transient neutrophil response in the low-dose groups, and presence of small granulomatous lesion and persistent neutrophil infiltration in the high-dose groups. In the inhalation study, rats were exposed to 0.37 mg/m³ aerosols of well-dispersed MWCNTs (>70% of MWCNTs were individual fibers) for 4 weeks, and were sacrificed at 3 days, 1 month, and 3 months after the end of exposure. The inhalation exposures delivered less amounts of MWCNTs into the lungs, and therefore less pulmonary inflammation responses was observed, as compared to intratracheal instillation. The results of our study show that well-dispersed MWCNT can produce pulmonary lesions, including inflammation.

Keywords: Nanomaterial, carbon nanotube, inhalation, intratracheal instillation, dispersion

Introduction

Multi-walled carbon nanotubes (MWCNTs) are a substance with many graphene sheets arranged concentrically. MWCNTs have superior thermal conductivity, electrical conductivity and mechanical strength. They hold promise for many applications including catalyst, cleaning methods, gene therapy, energy device materials, energy storage materials including hydrogen, composite resin materials and television electron emitters (Endo 1988; Iijima 1991). Many of the *in vivo* animal experimental research and

in vitro cell culture studies have been conducted to assess the potential effects of MWCNTs on humans (Mitchell et al. 2007; Card et al. 2008; Pacurari et al. 2008; Muller et al. 2009; Kobayashi et al. 2010; Rutishauser et al. 2010; Vankoningsloo et al. 2010). Much research shows MWCNTs to be toxic in *in vivo* and *in vitro* studies (Card et al. 2008; Pacurari et al. 2008), but some also show that MWCNTs are not toxic in *in vivo* studies (Mitchell et al. 2007; Muller et al. 2009; Kobayashi et al. 2010). Given the strong agglomeration of MWCNTs, it is considered that true responses of MWCNTs are masked, and that the formation of large agglomerates may lead to modify the responses in *in vivo* and *in vitro* studies (Kreyling et al. 2009; Liu et al. 2009; Morimoto et al. 2010a). Animal exposure studies show that giant particles formed by agglomeration in the trachea and lungs, easily leading to suffocation death (Warheit et al. 2004; Muller et al. 2005), a result differing both qualitatively and quantitatively from previous animal experiments (Lam et al. 2004; Shvedova et al. 2005).

There are many reports that agglomerated nanoparticles (NPs) induced the pulmonary inflammation which is not observed with micron-size particles at the same mass dose (Oberdörster et al. 2005; Card et al. 2008; Kobayashi et al. 2009). However, even if dispersed particles have been found in animal studies exposed to agglomerated NPs, it is likely that the effects of disperse particles could not be discerned due to their presence in only small fractions. In particular, agglomeration could diminish the effective dose of carbon nanotubes in the lungs. Researches show that individually dispersed carbon nanotubes have stronger bacterial toxicity than agglomerated nanotubes (Liu et al. 2009), and that dispersed single-walled carbon nanotubes (SWCNTs) stimulate more proliferation of bronchial epithelial cell than non-dispersed SWCNTs (Wang et al. 2010). Considering these

facts, it is significant to evaluate the toxicity of dispersed NPs, particularly individually dispersed NPs.

In intratracheal instillation studies and inhalation studies for evaluating the harmfulness of manufactured nanomaterials, research generally focuses on inflammation, fibrosis and cytotoxicity. In particular, inflammation centered on a neutrophil is related to lung disorder caused by asbestos, silica or metal NPs (Borm and Driscoll 1996; Shacter and Weitzman 2002, Nishi et al. 2009). Accordingly, in order to examine whether or not MWCNTs induce pulmonary toxicity, we developed an intratracheal instillation and inhalation animal exposure model to examine neutrophil infiltration in the lung.

Materials and methods

MWCNTs

MWCNTs were provided by Nikkiso Co., Ltd, Tokyo, Japan. The MWCNTs were synthesized by catalytic chemical vapor deposition (CVD) method.

Animals

Male Wistar rats (8 weeks old) were purchased from Kyudo Co., Ltd (Kumamoto, Japan). The animals were kept in the Laboratory Animal Research Center of University of Occupational and Environmental Health for a week with access to free-feeding of commercial diet and water. All procedures and animal handling were performed according to the guidelines described in the Japanese Guide for the Care and Use of Laboratory Animals as approved by the Animal Care and Use Committee, University of Occupational and Environmental Health, Japan.

Preparation of MWCNT suspensions

Solidified body of MWCNTs kneaded with fructose was ground using a planetary ball mill (P-6, Fritsch, Germany) for 20 min. After soaking the ground product in hot water for 24 h, the MWCNTs were separated from fructose by filtration and rinsing. Recovered MWCNTs were dispersed in a dispersing medium (an aqueous suspension of 0.5 mg/mL Triton X-100). Furthermore, the MWCNTs suspension was treated by hydrogen peroxide to remove fructose from MWCNTs surface completely. After heating the suspension, the MWCNTs were filtered with a membrane filter of 1 μm . The MWCNTs on the filter were re-dispersed into a dispersing medium by ultrasonication for 30 min using a homogenizer (Model 450, Branson, USA). The suspension of MWCNTs classified by centrifugation between 3,000 and 20,000 g was supplied for the *in vivo* tests after the content of MWCNTs in the suspension have been adjusted. These MWCNT suspensions were used in the intratracheal instillation study and for aerosolization in the inhalation study.

Characterization of MWCNT

For the bulk MWCNTs and dispersed MWCNTs in the testing suspension, tube morphology was evaluated on the basis of observations using a transmission electron microscope (TEM; JEM-1010; Jeol Ltd, Tokyo, Japan) at the acceleration voltage of 100 kV. Further, energy-filtering TEM observation

was performed with an EM922 (Carl Zeiss SMT, Germany), which was equipped with an OMEGA energy filter. Zero-loss filtering, which can increase the scattering and phase contrast of the TEM image, was carried out. The Brunauer, Emmett, Teller (BET) specific surface area of the bulk MWCNTs was measured by the N_2 gas adsorption method (Autosorb-1-C; Quantachrome Instruments, USA). The metal impurities of the bulk MWCNTs were determined by quantitative analysis of 28 elements with inductively coupled plasma-mass spectrometer (ICP-MS; Agilent Technologies 7500a, Tokyo, Japan) after microwave assisted acid digestion of the CNTs. In order to evaluate the degree of MWCNT damage upon sample preparation, the presence of defects in the graphene structure of the bulk MWCNTs and the MWCNT suspensions was evaluated by Raman spectroscopy (Nicolet Almega XR micro-Raman system; Thermo Fisher Scientific Inc., Japan) and powder X-ray diffraction (XRD; PW-1800, Philips Electronics, The Netherlands). The resonance Raman scattering spectra were measured in the frequency regions of 100–1800 cm^{-1} with an excitation wavelength of 532 nm. Furthermore, functionalization of MWCNT surface by sample the preparation was checked by X-ray photoelectron spectroscopy (XPS; VG Theta Probe, Thermo Fisher Scientific Inc., USA).

Intratracheal Instillation of MWCNT

A total of 0.2 mg (0.66 mg/kg) or 1 mg (3.3 mg/kg) of MWCNTs was suspended in 0.4 mL of distilled water including 0.05% Triton X. Each material suspension was intratracheally instilled once in Wistar male rats (9 weeks old). The negative control group was exposed to distilled water including 0.05% Triton X. The animals were dissected at 3 days, 1 week, 1 month, 3 months, and 6 months after instillation.

Inhalation study of MWCNT

The whole-body exposure system, used to expose rats to the MWCNT suspended in air, consisted of a pressurized nebulizer and a mist dryer and was connected to an exposure chamber (volume: 0.52 m^3). The MWCNT suspension prepared for the intratracheal instillation study was also used for the inhalation study. The suspension was put into the nebulizer and used for the generation of MWCNT aerosols. The size distribution (electrical mobility equivalent diameter distribution) of the MWCNT aerosol and Triton X aerosol particles at the exit of the nebulizer and inside the exposure chamber were measured repeatedly using a particle spectrometer consisting of a differential mobility analyzer and a condensation particle counter (DMA-CNC, Model 1000XP WPS, MSP Corp., Shoreview, MN, USA) to monitor the stability throughout the exposure period. The MWCNTs in the chamber were collected with a 0.2 μm polycarbonate filter and observed by scanning electron microscopy (SEM, Hitachi S-4500). The diameter and length of the MWCNT were measured with the SEM microphotograph, and the geometric mean diameter (geometric standard deviation, GSD) and geometric mean length (GSD) were 63 nm (1.5) and 1.1 μm (2.7), respectively. The MWCNT and Triton X aerosol in the chamber were collected with quartz fiber filter (QAT-UP, Pall, USA), the elemental carbon amounts were

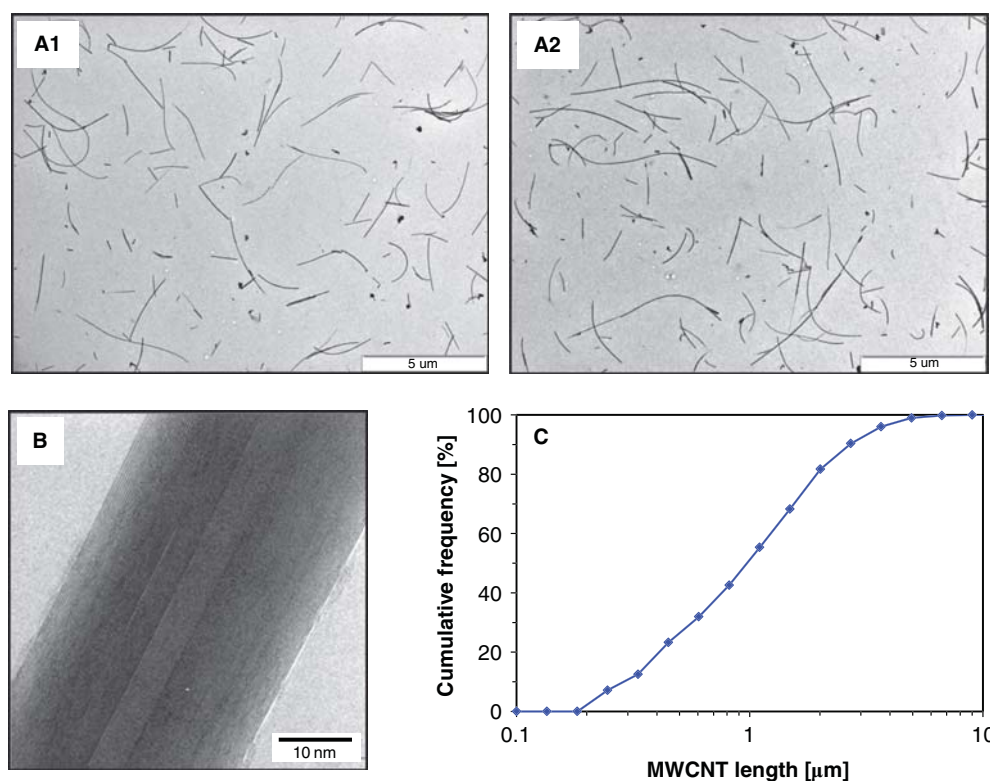


Figure 1. Morphology of the MWCNTs dispersed in the testing suspension. (A1 & 2) Transmission electron microscopy (TEM) images of MWCNTs at low magnifications. Almost all of the MWCNTs are individually dispersed in the suspension. (B) TEM image of MWCNTs at high magnification. Well-crystalline structure of the tube walls can be seen in the image. (C) Distribution of MWCNT length on the basis of TEM observation. After a measurement of 1005 MWCNTs, geometric mean (and geometric standard deviation) of the length was determined to be 0.94 µm (2.3). Minimum and maximum lengths of the MWCNTs were 0.22 and 8.91 µm, respectively.

determined by an OC-EC Aerosol Analyzer (Sunset Laboratory, Forest Grove, USA), and the concentrations in the chamber were calculated. The daily average mass concentration of MWCNT in the chamber was $0.37 \pm 0.18 \text{ mg/m}^3$ (including Triton X : $0.47 \pm 0.18 \text{ mg/m}^3$) in the exposure period, respectively. The mean of geometric mean diameter

of Triton X aerosol in the chamber measured by SMPS during the inhalation was 52 nm.

Male Wistar rats (9 weeks old) were divided into three groups: MWCNT, Triton X, and unexposed. Rats were exposed to the aerosol for 6 h a day, 5 days a week, for 4 weeks in a whole-body exposure chamber. The unexposed

Table I. Characterization of multi-walled carbon nanotubes (MWCNTs).

Characteristic	Value	Measuring method
Bulk MWCNTs		
Diameter ^a	44 nm (1.3)	Scanning electron microscopy (SEM) observation
BET surface area ^b	$69 \pm 37 \text{ m}^2/\text{g}$	N ₂ adsorption method
D/G ratio	0.078	Raman spectroscopy analysis
Half width of the peak at 25.60° ^c	1.01°	X-ray diffraction (XRD) analysis
Metal content		
Li	0.5 ppm	Inductively coupled plasma - mass spectrometry (ICP-MS) analysis
Al	80 ppm	
Ca	176 ppm	
Fe	53 ppm	
Cd	16 ppm	
Dispersed MWCNTs in solution		
Diameter ^a	48 nm (1.1)	Transmission electron microscopy (TEM) observation
Length ^a	0.94 µm (2.3)	Transmission electron microscopy (TEM) observation
D/G ratio	0.174	Raman spectroscopy analysis
Half width of the peak at 25.60° ^c	0.93°	X-ray diffraction (XRD) analysis
MWCNT aerosol in exposure chamber		
Diameter ^a	63 nm (1.5)	Scanning electron microscopy (SEM) observation
Length ^a	1.1 µm (2.7)	Scanning electron microscope (SEM) observation
Mass concentration ^b	$0.37 \pm 0.18 \text{ mg/m}^3$	OC-EC Aerosol Analyzer

^aValues are expressed as geometric mean (geometric standard deviation); ^bValues are expressed as mean \pm SD; ^cCorresponding to the {0 0 3} plane of synthetic carbon/graphite [JCPDS Card #: 26-1079].

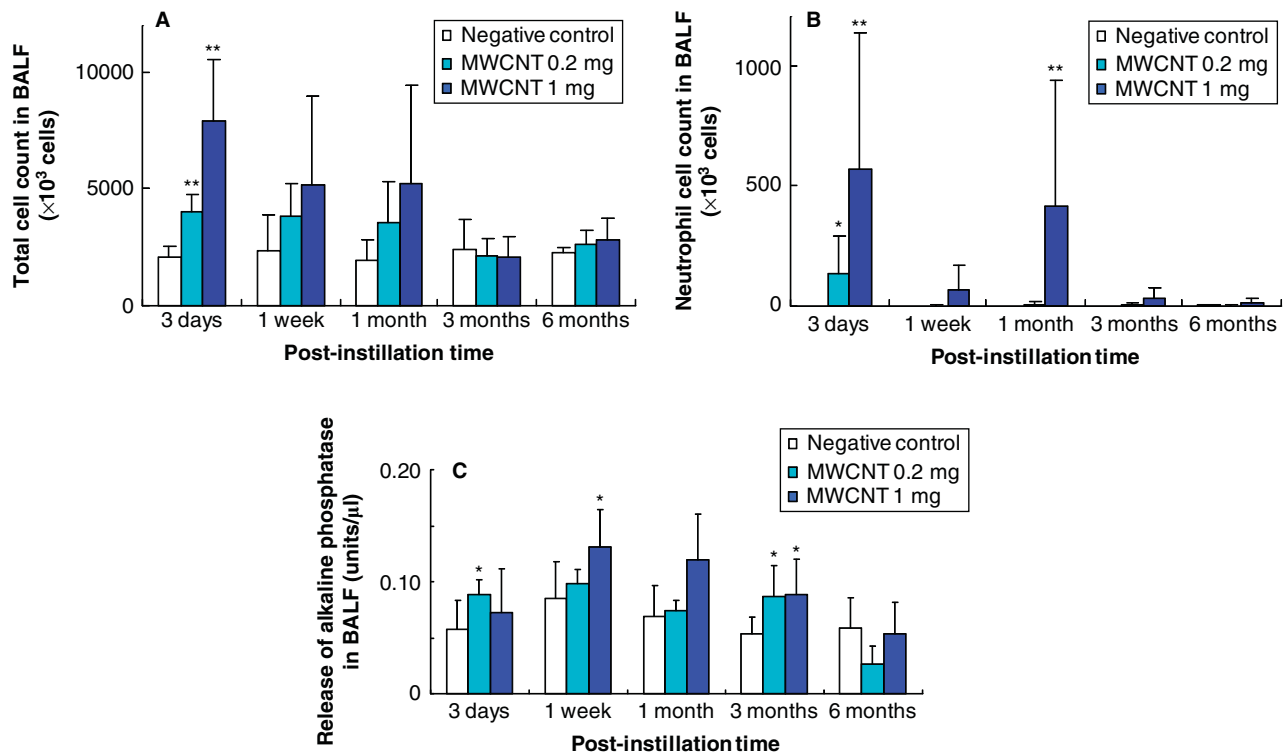


Figure 2. BALF results after intratracheal instillation of MWCNT. (A) Total cell count. (B) Neutrophil cell count. (C) Release of alkaline phosphatase (ALP). Each column and bar represents the mean \pm standard deviation of five rats. An asterisk indicates a statistically significant difference of $p < 0.05$ compared to each negative control group; double asterisk, of $p < 0.01$ compared to each negative control group. Intratracheal instillation of MWCNT induced inflammatory response and injury in the lung.

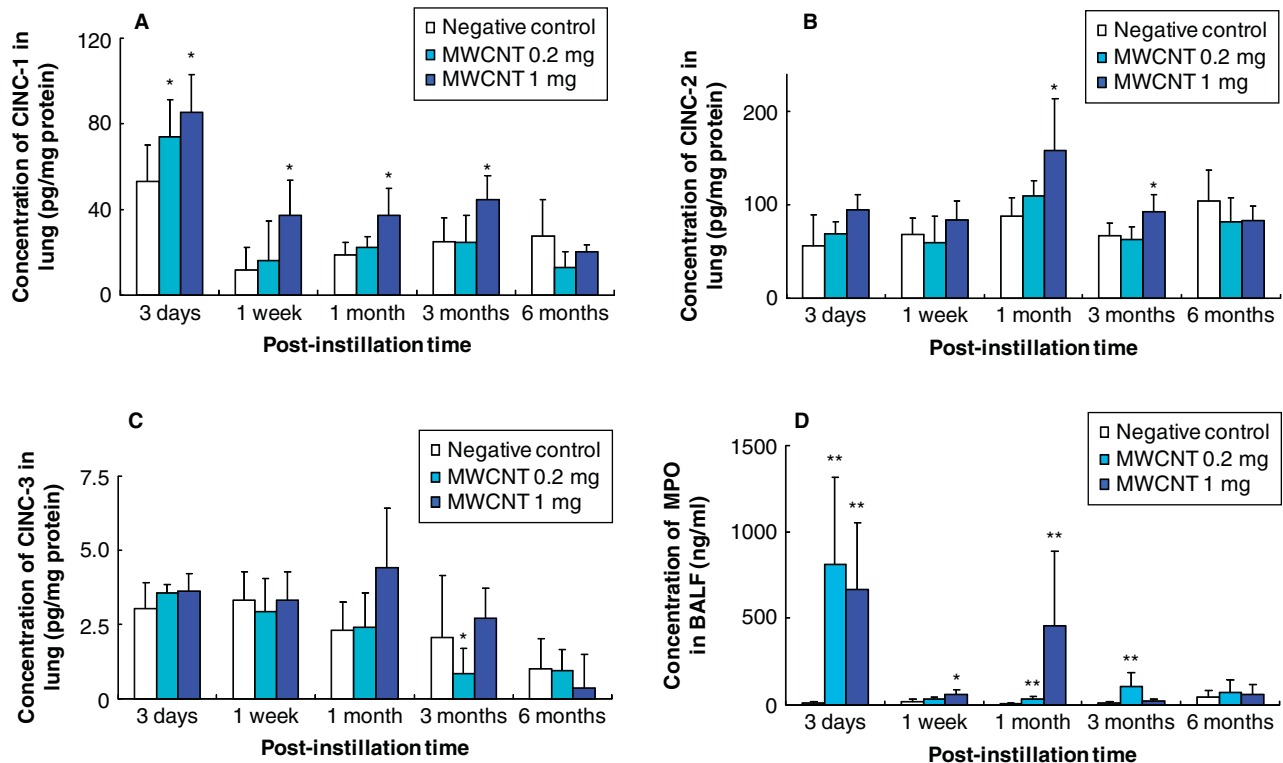


Figure 3. Concentration of CINC in rat lungs and concentration of myeloperoxidase in BALF after intratracheal instillation of MWCNT. (A) CINC-1. (B) CINC-2. (C) CINC-3. (D) Myeloperoxidase. Each column and bar represents the mean \pm standard deviation of five rats. An asterisk indicates a statistically significant difference of $p < 0.05$ compared to each negative control group; double asterisk, of $p < 0.01$ compared to each negative control group. A high dose of MWCNTs induced a persistent increase of CINC-1, and a low dose of MWCNTs induced a transient increase.

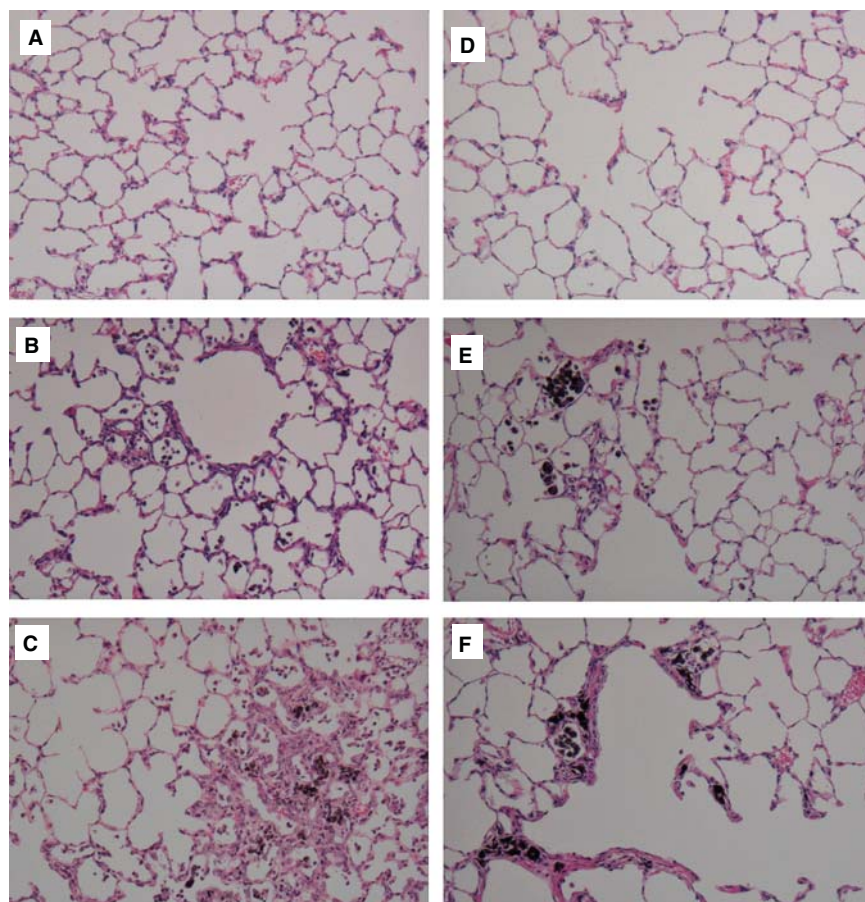


Figure 4. Hematoxylin and eosin staining of lung sections after intratracheal instillation of MWCNT. Magnification $\times 100$. (A) Lung of negative control at 3 days; (B) 0.2 mg MWCNT-exposed lung at 3 days; (C) 1 mg MWCNT-exposed lung at 3 days; (D) Lung of negative control at 3 months; (E) 0.2 mg MWCNT-exposed lung at 3 months; (F) 1 mg MWCNT-exposed lung at 3 months. Persistent inflammation was found in lung tissue in the 1 mg MWCNT-exposed groups. Mild inflammation and no granulomatous lesions were found in lung tissue in the 0.2 mg MWCNT-exposed groups at the acute phase.

rats were exposed to only clean air in a same-sized chamber located in the same air-conditioned room. Triton-exposed rats as negative control were designed to inhale Triton X aerosol particles, prepared by using Triton X suspension and another set of nebulizer and mist dryer. The daily average mass concentration of Triton X in the chamber was $0.08 \pm 0.01 \text{ mg/m}^3$ in the exposure period. After exposure for 4 weeks, rats were dissected at 3 days, 1 month, and 3 months of recovery.

Animals after inhalation and intratracheal instillation studies

Each group of 10 animals was divided into two subgroups of five animals for lung tissue analysis. The first subgroup (five rats) provided bronchoalveolar lavage, which was collected using physiological saline that was injected through a cannula inserted in the respiratory tract, into the right lung, while the left lung was clamped. Three to 10 mL (different volumes of lavage fluid are based on animal ages) of physiological saline was infused in the right lung each time and lavage fluid was collected up to 50 mL in total. On the other hand, the left lung was inflated and fixed by 4% paraformaldehyde at 25 cm H_2O pressure. The lungs of the second subgroup (five rats) were homogenized to extract protein.

Chemokine measurement of lung tissue and BALF

Lung tissue was homogenized with a T-PER tissue protein extraction reagent, and then centrifuged (1500 g for 10 min). The protein concentration of the supernatant was measured by the BCA Protein Assay Kit (PIERCE) using Bovine serum albumin as a standard. Total protein concentration was adjusted with a final concentration of 500 $\mu\text{g/ml}$ for cytokine-induced neutrophil chemoattractant-1 (CINC-1) and CINC-2 and 4000 $\mu\text{g/ml}$ for CINC-3. Chemokine concentration was determined by Quantikine Rat CINC-1, CINC-2, and CINC-3 (R&D Systems) (Cat. #RCN100, #RCN200, and #RCN300, respectively) and absorbance at 450 nm was measured by a microplate reader. CINC-1, CINC-2, and CINC-3 in the lung tissue were determined. Alkaline phosphatase (ALP) and myeloperoxidase (MPO) released in the BALF supernatant was determined by LabAssayTM ALP (Wako Pure Chemical Industries, Ltd, Japan) and Rat MPO ELISA KIT (Hycult Biotech, The Netherlands), respectively.

Tissue preparation for HE stain

The lungs, which were inflated and fixed by 4% paraformaldehyde, and trachea were resected from the surrounding tissue. The lung tissue was embedded in paraffin, and 5 μm -thick sections were cut from the lobe. The samples were then sectioned and stained with hematoxylin and eosin.

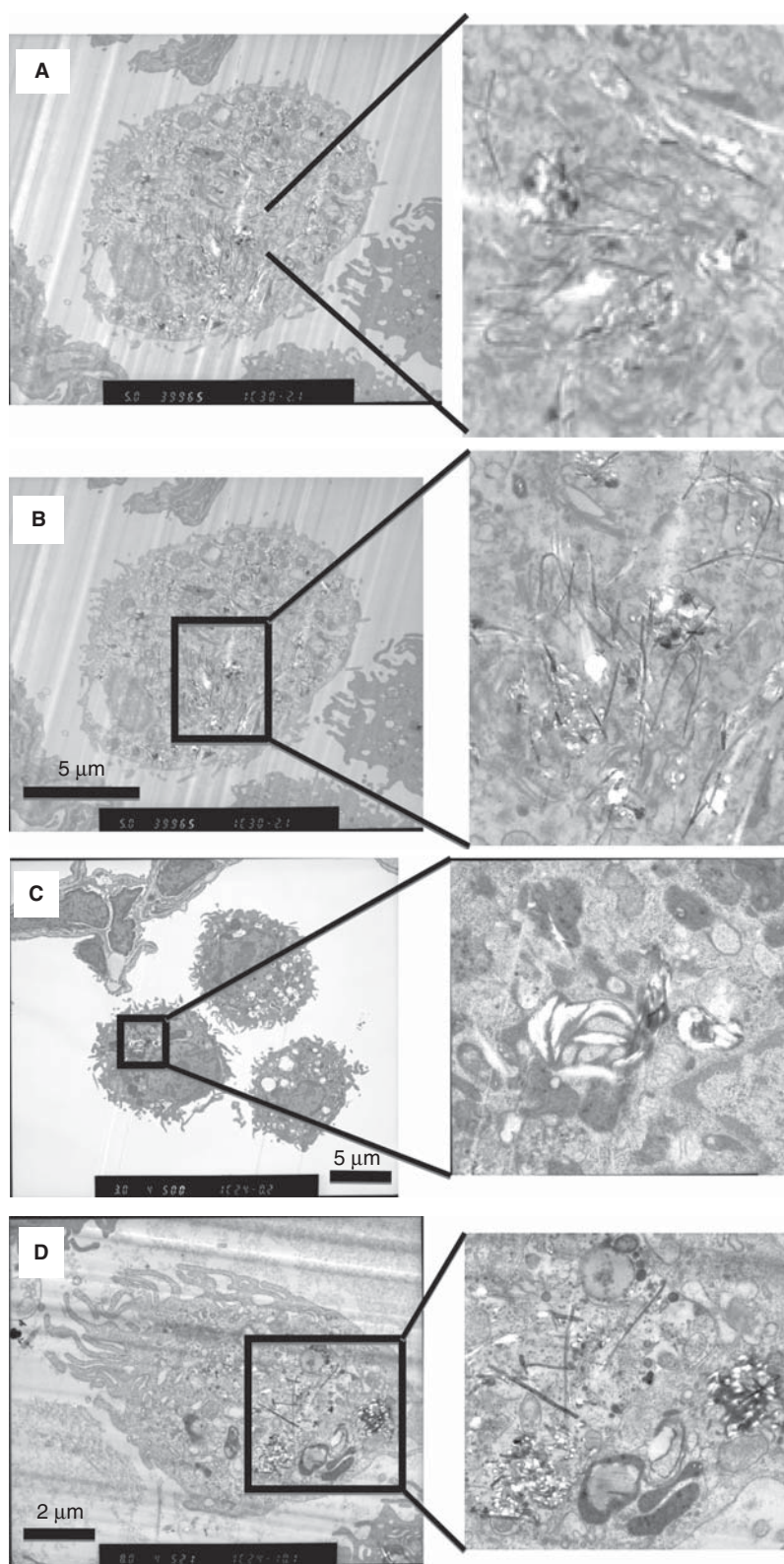


Figure 5. Alveolar macrophages in 0.2 mg MWCNT-exposed lung using TEM at 1 month after intratracheal instillation of MWCNTs. (A) 0.2 mg MWCNT-exposed lung at 1 month; (B) 1 mg MWCNT-exposed lung at 1 month; (C) 0.2 mg MWCNT-exposed lung at 6 months; (D) 1 mg MWCNT-exposed lung at 6 months; (E) Structure of MWCNT in 1 mg-exposed lung at 1 month; (F) Structure of MWCNT in 1 mg-exposed lung at 6 months. Dispersed MWCNTs were also identified in the alveolar macrophage. The denature of MWCNTs was not observed during observation times.

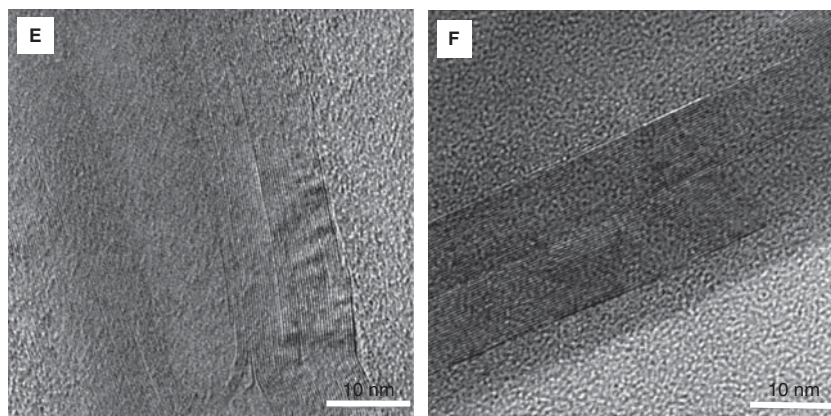


Figure 5. (Continued).

Processing of lung tissue for transmission electron microscope (TEM)

The lung tissues were fixed using glutaraldehyde and osmium tetroxide solution, and then dehydrated in ethanol, and embedded in epoxy resin. The specimens were stained with a 2% uranyl acetate solution and 0.5% lead citrate solution at room temperature. Conventional TEM observation was performed within an H-7000 (Hitachi, Japan) at the acceleration voltage of 80 kV. Energy-filtering TEM observation was performed with an EM922 (Carl Zeiss SMT, Germany), which was equipped with an OMEGA energy filter. Zero-loss filtering, which can increase the scattering and phase contrast of the TEM image, was carried out.

Statistical analysis

Statistical analysis was carried out using the Mann-Whitney test with differences of $p < 0.05$ considered to be statistically significant.

Results

Characterization of MWCNT (Figure 1, Table I)

Fundamental characteristics of the bulk MWCNTs, dispersed MWCNTs in the testing suspension, and MWCNT aerosol in

exposure chamber are summarized in Table I. Based on the TEM observations, geometric mean (and geometric standard deviation) of the diameter of bulk MWCNTs was determined to be 44 nm (1.3). Specific surface area was determined to be $69 \pm 37 \text{ m}^2/\text{g}$ (mean \pm SD) by BET method. The individual metal content determined by ICP-MS demonstrated that high purity of the bulk MWCNT material with little incorporation of metal catalyst particles that were used in the manufacturing process.

Generally, intense dispersion processes of MWCNTs into vehicles can cause degradation in MWCNT quality by introducing defects in the crystalline structure of MWCNTs. A convenient measure to evaluate the degradation in MWCNT quality is the 'D/G ratio', the ratio of the intensities of disorder-induced mode (D-band) and graphene-induced mode (G-band), which appears in the Raman spectrum (Dillon et al. 2005; Dresselhaus et al. 2005; Lee et al. 2008; Musumeci et al. 2008). The D/G ratios of the bulk material and the dispersion suspension were estimated to be 0.078 and 0.174, respectively, suggesting that there was a slight drop in MWCNT quality of the dispersion suspension. However, a half width of the peak at 2θ of 25.60° in XRD spectrum, which corresponds to the $\{0\ 0\ 3\}$ plane of synthetic carbon/graphite [JCPDS Card #: 26-1079] (i.e., disturbance in the interlayer spacing of MWCNT walls), was not significantly changed upon sample preparation (from $1.01\text{--}0.93^\circ$), suggesting that overall damage of MWCNTs upon sample preparation was not significant (Darsono et al. 2008). Furthermore, atomic ratio of oxygenated groups on the MWCNT surface was preliminarily estimated from the XPS analysis (method similar to Wepasnick et al. 2010). For the bulk MWCNTs, the ratios of C-O, C=O, and COOH functions were 7.3, 3.0, and 2.6 atomic %, respectively. Oxygen/carbon atomic ratio calculated from proportion of C1s and O1s peak areas on the XPS spectra was 0.004. For the dispersed MWCNTs, the ratios of C-O, C=O, and COOH were 7.8, 2.9, and 0.8 atomic %, respectively. Oxygen/carbon atomic ratio was 0.01. Thus the change in surface modification is estimated to be small although a slight increase in oxygen content was observed, suggesting an influence of oxidation or functionalization during the dispersing process.

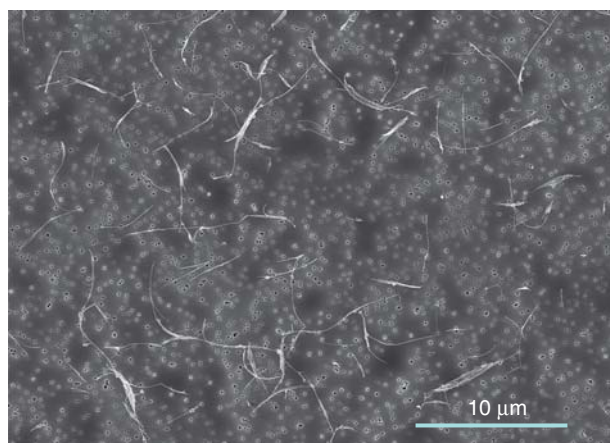


Figure 6. Transmission electron micrograph image of MWCNTs in alveolar macrophages. About 70% of the MWCNT fibers are individually dispersed.

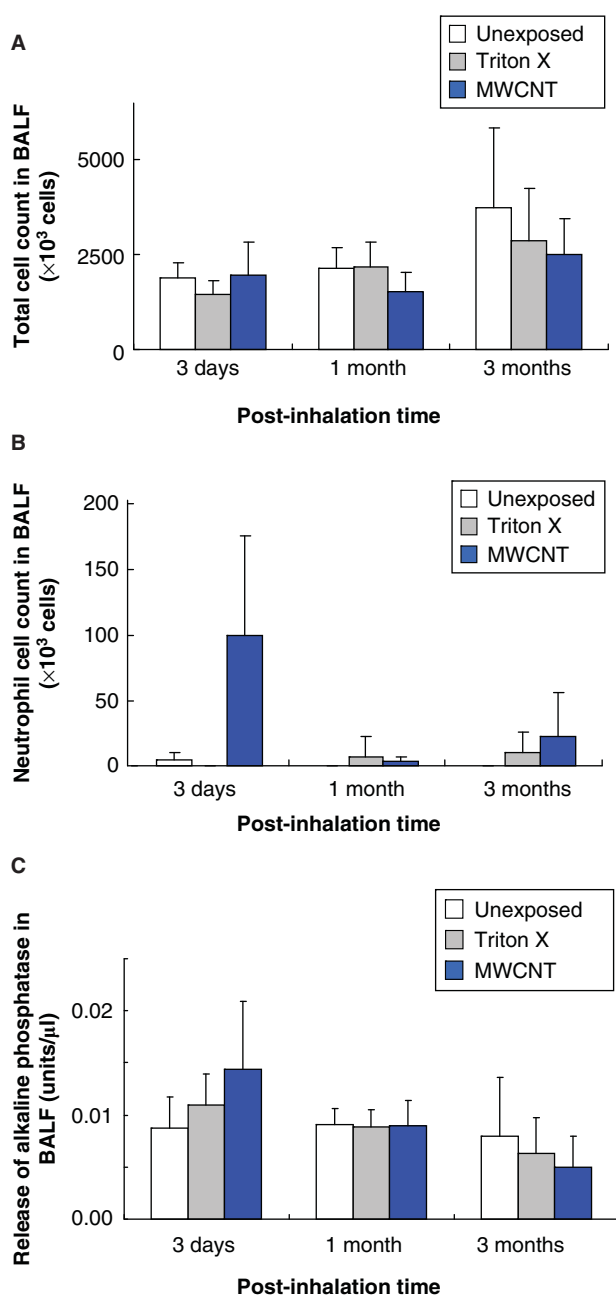


Figure 7. BALF results after inhalation of MWCNT. (A) Total cell count; (B) Neutrophil cell count. (C) Release of ALP. Each column and bar represents the mean \pm standard deviation of five rats. An asterisk indicates a statistically significant difference of $p < 0.05$ compared to each unexposed group; double asterisk, of $p < 0.01$ compared to each unexposed group. Inhalation of MWCNT induced the transient inflammatory response in rat lungs.

In the testing suspensions, MWCNTs were present as they are individually dispersed (Figure 1A). Furthermore, well-crystalline structure of the tube walls can be seen in the TEM image at high magnification (Figure 1B), supporting the results of XRD analysis. The diameter and length (Figure 1C) of the MWCNTs in the suspension were measured from TEM images. After a measurement of 1005 MWCNTs, geometric mean (and geometric standard deviation) of the diameter and length were determined to be 48 nm (1.1) and 0.94 μ m (2.3), respectively. Minimum and maximum lengths of MWCNTs were 0.22 and 8.91 μ m, respectively.

Intratracheal instillation study

Cell count and ALP release in BALF

Figure 2A–B shows the number of total cells and neutrophils in BALF. In comparison with the negative control group (0.05% Triton X in distilled water), the total cell count was significantly increased in MWCNT 0.2 mg and 1 mg groups at 3 days after intratracheal injection. Significant increases of the neutrophil count were also found at 3 days and 1 month in the MWCNT 1 mg group; a transient increase was found at 3 days in the MWCNT 0.2 mg group. Figure 2C showed the amount of released alkaline phosphatase in BALF. Significant increases were observed at 1 week and 3 months in the MWCNT 1 mg group, and at 3 days and 3 months in the MWCNT 0.2 mg group.

CINC concentration in lung and MPO concentration in BALF (Figure 3A–D)

The concentration of CINC-1 in lung tissue persistently increased from 3 days to 3 months in the 1 mg MWCNT group compared with that in the negative control group. Meanwhile, the 0.2 mg MWCNT group only revealed a temporary increase at 3 days. Regarding the CINC-2 concentration, there were significant increases at 1 month and 3 months in 1 mg MWCNT groups. In the 0.2 mg MWCNT group, a significant increase was not found throughout the observation period.

As for CINC-3 concentration, there were not significant increases in either the 0.2 or 1 mg MWCNT group. The MPO concentration showed significant increases over the negative control from 3 days to 1 month in the 1 mg MWCNT group; significant increases in MPO were found at 3 days, 1 month and 3 months in the 0.2 mg group.

Histopathological changes in lungs (Figure 4)

In the group to which 1 mg of MWCNT was administered, neutrophils, eosinophils and alveolar macrophages were constantly infiltrating from alveolar ducts and alveolar spaces to terminal bronchioles. This continued for at least 6 months, although the extent of infiltration decreased as time elapsed during the observation period. However, at the 3 and 6 months, neutrophils and eosinophils were almost not observed; infiltration was mainly by alveolar macrophages. Small granulomatous lesion and transient collagen deposition were also observed. Regarding the group to which 0.2 mg of MWCNT was administered, granulomatous lesions were not observed. Only slight and transient infiltration of inflammatory cells was observed.

Morphological feature of alveolar macrophage by TEM

In an alveolar macrophage, MWCNT was observed in phagolysosomes. This trend was particularly pronounced in the group to which 1 mg of MWCNT was administered. While some MWCNTs agglomerated inside phagolysosomes, some MWCNTs also existed independently. However, MWCNTs were not found in the nucleus or in organelles, including the group to which high dose was administered. Figure 5E and 6F show the expanded graphs of MWCNT. As for internal structure, the multilayer structure was maintained; degradation was not observed.

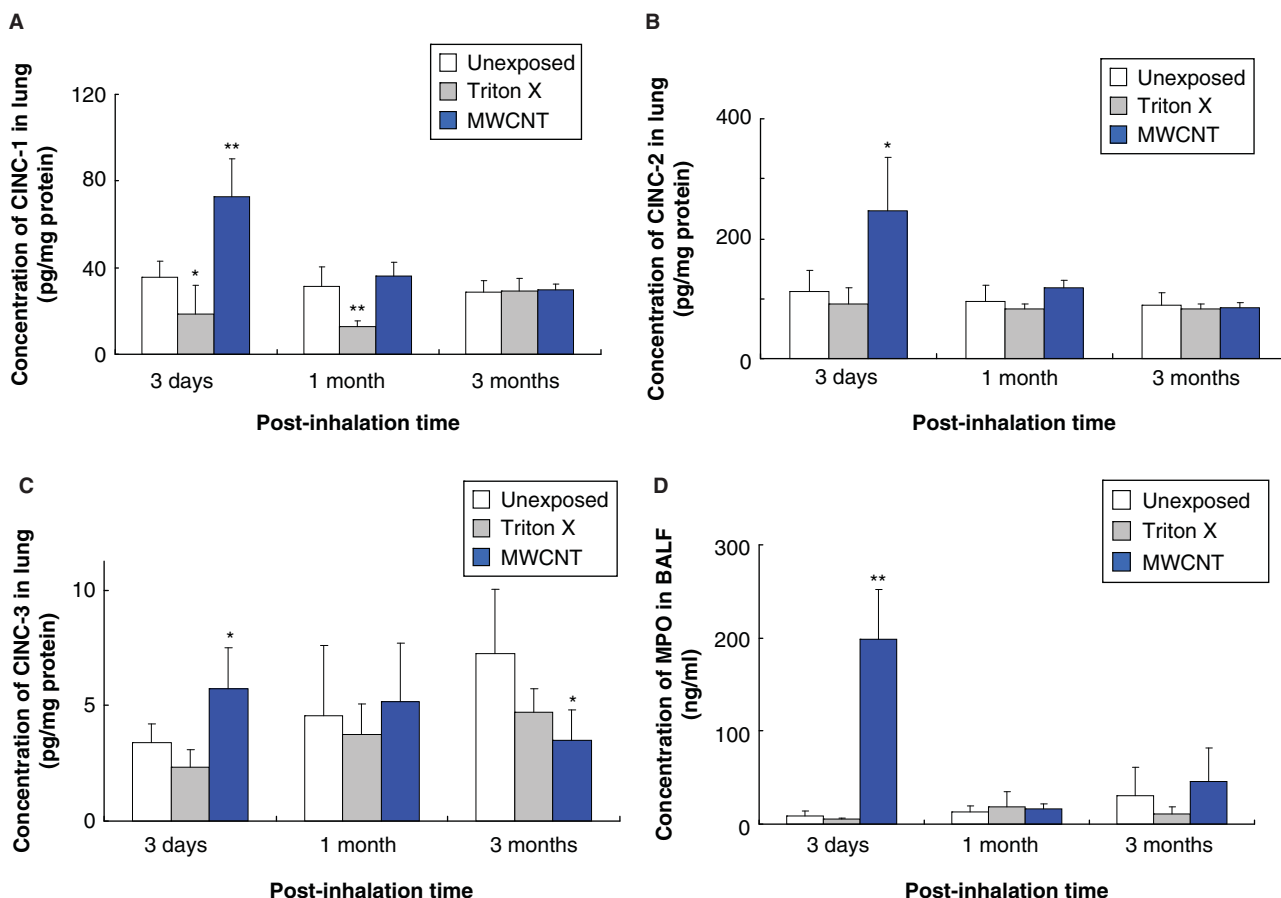


Figure 8. Concentration of CINC in rat lungs and concentration of myeloperoxidase in BALF after inhalation of MWCNT. (A) CINC-1; (B) CINC-2; (C) CINC-3; (D) Myeloperoxidase. Each column and bar represents the mean \pm standard deviation of five rats. An asterisk indicates a statistically significant difference of $p < 0.05$ compared to each unexposed group; double asterisk, of $p < 0.01$ compared to each unexposed group. Inhalation of MWCNT transiently induced concentration of CINC-1, CINC-2, and CINC-3.

Inhalation study

Figure 6 shows an image of MWCNTs in the rat chamber obtained by TEM. About 70% of the MWCNT fibers are maintained individually, 20% in bundles of 2 or 3 intertwined fibers. About 10% are in tangles that indicate discrete masses.

Cell count and ALP release in BALF

Figure 7 shows the total cell and neutrophil counts in BALF. There was no significant difference in the total cells among the unexposed group, the Triton group and the MWCNT group. Although the MWCNT group showed the increasing tendency at 3 days, there was also no significant difference in the neutrophils counts among the three groups. Significant increase in ALP release in BALF in the MWCNT group was not observed through the observation period.

CINC concentration in lung and MPO concentration in BALF (Figure 8A–D)

The concentration of CINC-1 in lung tissue in the MWCNT group was significantly increased over the unexposed group at 3 days. The Triton group showed significant decreases at 3 days and 1 month, reaching the same level as the unexposed group 3 months later. Regarding the CINC-2 concentration, the MWCNT group showed a significant increase over the unexposed group at 3 days. As for the CINC-3 concentration in lung tissue, the MWCNT group also showed

a significant and transient increase over the unexposed group at 3 days. As for the MPO concentration, the MWCNT group also showed a significant increase over the unexposed group at 3 days.

Histopathological changes in lungs (Figure 9)

In an MWCNT exposure group, neutrophil infiltration into alveolar space, granulomatous lesion, or interstitial collagen deposition was not found during the observation period. However, although only to a slight extent, alveolar macrophages that ingested MWCNT were observed. Even in the Triton group, the result was practically the same as for the unexposed group and nothing unusual was observed throughout the period.

Morphological feature of alveolar macrophage by TEM (Figure 10)

In an alveolar macrophage, MWCNT was found in phagolysosomes. Some of the MWCNT was agglomerated, but some was individual. MWCNT was not observed in nuclei or organelles.

Discussion

The MWCNTs used in the intratracheal instillation and inhalation studies are the same material, and both were

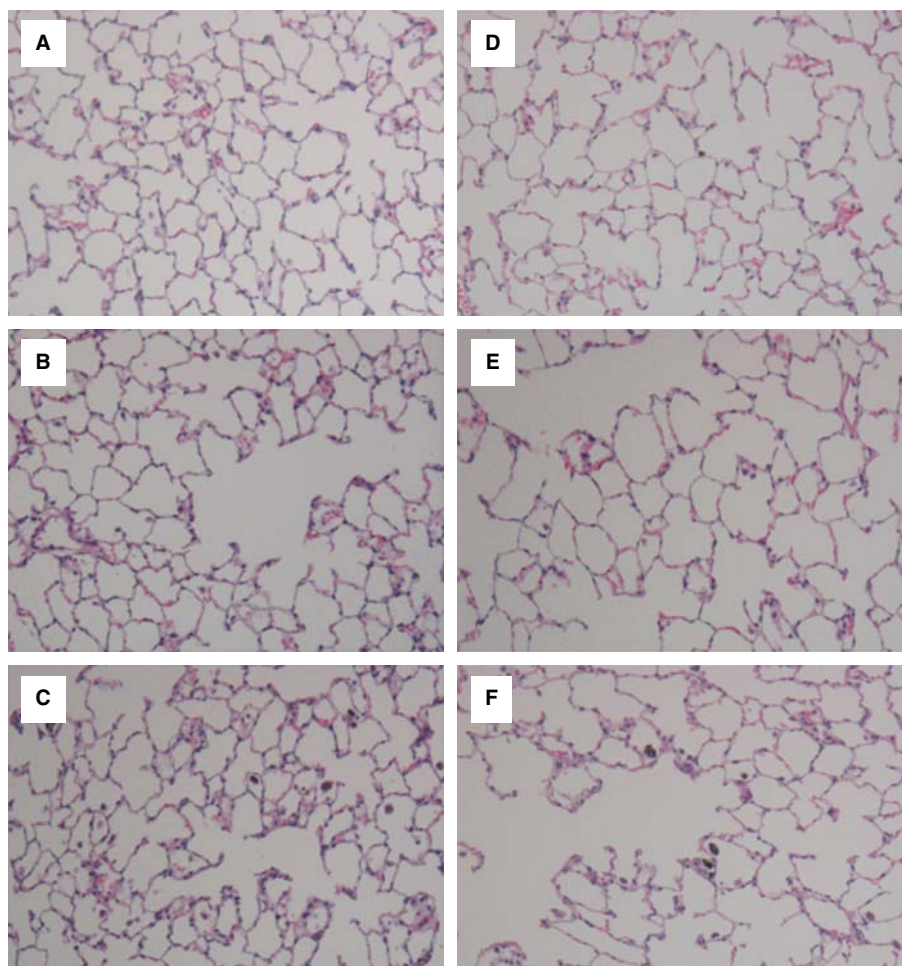


Figure 9. Hematoxylin and eosin staining of lung sections after inhalation of MWCNT. Magnification $\times 100$. (A) Unexposed lung at 3 days; (B) Triton-exposed lung at 3 days; (C) MWCNT-exposed lung at 3 days; (D) Unexposed lung at 1 month; (E) Triton-exposed lung at 1 month; (F) MWCNT-exposed lung at 1 month. Minimum transient inflammatory response was observed in MWCNT-exposed lungs.

prepared by the same solidified-milling technique. Our sample preparation procedure kept the crystalline structure of MWCNTs, suggesting that MWCNTs were not significantly degraded upon the preparation. In addition, the TEM observation of MWCNTs in the intratracheal instillation study and inhalation study revealed that the former is individual, while the latter is 70% individual. Accordingly, we think that we could evaluate the pulmonary toxicology of well-dispersed MWCNTs in the present studies.

In this intratracheal instillation study, low doses of MWCNTs caused transient inflammation in the lung. The inflammatory cells, mainly neutrophils, were infiltrating from alveolar spaces and alveolar ducts into terminal bronchioles. Granulomatous lesions were not observed at low dose level. In many reports, granulomas or granulomatous lesions are observed immediately after the intratracheal instillation (Muller et al. 2008a, 2008b; Mutlu et al. 2010). We speculate that dispersed fibers hardly induce the granulomatous formation at low dose. Muller et al. (2005) reported that in intratracheal instillation study of ground MWCNTs, it disperses widely into pulmonary parenchyma and causes inflammation, while in intratracheal instillation studies of raw material of MWCNT it forms granulomas around large agglomerations in the trachea. It has also reported that in an

aspiration study of dispersed SWCNT, granulomatous lesions are not found in the lungs but interstitial fibrosis is caused, and that when the SWCNT is not dispersed, granulomatous lesions are found in lung tissue (Mercer et al. 2008). On the other hand, at high doses of MWCNTs, the inflammatory cells infiltrated into the same sites and granulomatous lesions were also found. We consider that this granulomatous formation was observed in the early stages at the high dose, which seems to be due to the bolus effect. Since MWCNTs were injected at a dose of 1 mg, nearly an overdose, an artifact might occur. However, most of the granulomatous lesions were small.

MWCNTs were found for up to 6 months although they were decreasing in the lung. Pulmonary clearance of the MWCNTs used in the study may be poor due to low solubility with high purity of the inorganic matter (carbon). There was no structural degradation at 6 months after intratracheal injection. We think that the main clearance of the MWCNTs may be the clearance by alveolar macrophage. MWCNTs were also observed in phagolysosomes in alveolar macrophages in the present studies.

High dose of the MWCNTs produced persistent expressions of CINC-1 and CINC-2 among CINC. We prepared an animal model in which low dose (0.2 mg) nickel oxide NPs of

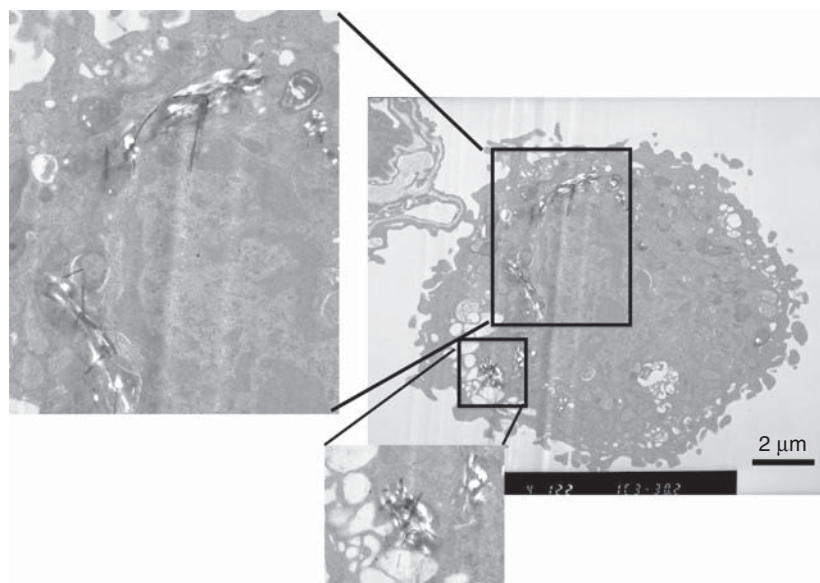


Figure 10. Alveolar macrophages in MWCNT-exposed lungs using TEM at 1 month after inhalation. MWCNT-exposed lung. Dispersed MWCNTs were also identified in the alveolar macrophage.

agglomeration size on the nanoscale were injected intratracheally, and observed persistent inflammation of neutrophils in the lung tissue and persistent increase of expressions of CINC-1 and 2 (Nishi et al. 2009). In lung injury models of diesel particles and hair spray, which are known to be harmful to lungs, increase of expressions of CINC-1 has been reported (Mitsunashi et al. 1999; Yokota et al. 2005). Compared with the results of intratracheal instillation of titanium dioxide (micron size), and dispersed fullerene NPs (Nishi et al. 2009; Morimoto et al. 2010b), which are relatively harmless to lungs, inflammation remained at a minimum, and expressions of CINC-1 and 2 remained at a transient mild increase typical of the acute period. These findings suggest an association between pulmonary neutrophil infiltration and CINC expression in the present study. In our model of neutrophil inflammation by NPs in an intratracheal instillation study, we performed a lung tissue microarray and analyzed the gene expression profile, and found that the CINC family was upregulated among the chemokine (Fujita et al. 2009).

Injury to alveolar epithelial cells will conceivably play a part in inflammation and fibrosis in the lungs. In order to examine if NPs contribute to lung injuries, we examined their capability to release alkaline phosphatase from alveolar epithelial cells in the intratracheal instillation and inhalation studies. In the intratracheal instillation study, a significant amount of alkaline phosphatase released in BALF was found at a high dose of the MWCNT. We also found the pulmonary inflammation and the alkaline phosphatase release level increased in the intratracheal instillation study of nickel oxide NPs (Nishi et al. 2009; Morimoto et al. 2010c). For fullerene, which did not show inflammation or fibrosis, its release was not found (Morimoto et al. 2010b). Sayes et al. (2007) also found a significant amount of alkaline phosphatase in BALF in an intratracheal instillation study with crystalline silica; but did not find the same results in the study with fullerene. In this study MWCNTs showed

reactions similar to those of inflammation-inducing materials such as silica and nickel oxide. This suggests that the inflammation due to MWCNTs in this study may partially occur via alveolar epithelial cells.

The inhalation study showed that MWCNTs produce only minimal transient inflammation and no granulomatous lesions in the lung. Ma-Hock et al. (2009) exposed rats to inhalation of MWCNTs at exposure concentrations of 0.1, 0.5 and 2.5 mg/m³ for 13 weeks, and found an increase in pronounced multifocal granulomatous inflammation, diffuse histiocytic and neutrophil inflammation, and intra-alveolar lipoproteinosis in the lung tissue at 0.5 and 2.5 mg/m³. Minimal granulomatous inflammation occurs at a low concentration (0.1 mg/m³). In addition, Pauluhn (2010) conducted a 13-week inhalation study at exposure concentrations of 0.1, 0.4, 1.5 and 2.5 mg/m³. At 1.5 and 2.5 mg/m³ goblet cell hyperplasia, metaplasia, inflammatory changes in the bronchioalveolar region and increased interstitial collagen were observed. They reported that 0.4 mg/m³ was the borderline of neutrophilic inflammation and 0.1 mg/m³ is at NOAEL. Pulmonary responses of the rats exposed to 0.37 mg/m³ of MWCNTs in the present study were consistent with those of the previous studies. Furthermore, considering the dose of MWCNTs, pulmonary responses of our inhalation and intratracheal instillation studies were considered to be consistent. Pulmonary deposition of MWCNTs in lungs of rats can be calculated as follows. Assuming that the respiratory minute volume (RMV) of rat with approximately 0.3 kg body weight (BW) is 0.19 L/min based on the equation $RMV = 0.499 \times BW^{0.809}$, obtained by Bide et al. (2000), and the deposition fraction of inhaled MWCNT into the lungs of rats is 0.1 (10%) based on the study of Miller (2000), then pulmonary deposition of MWCNT is calculated to be approximately 50 μg through the exposure period. Therefore, there is a correspondence between our study results that no significant pulmonary inflammation was observed in the inhalation study with 50 μg of MWCNT pulmonary deposition and that

the transient pulmonary inflammation was observed in the intratracheal instillation study with 200 µg of MWCNT pulmonary deposition.

The MWCNTs used in the present inhalation study were short, 1.1 µm in geometric mean length and 63 nm in diameter. The short fibers were used for keeping specific surface area relatively large and producing chemically isolated fibers. Poland et al. (2008) administered 50 µg of CNT, asbestos and carbon black into a mouse abdominal cavity, and observed the effects 1 and 7 days later. With fibers longer than 15 µm, significant inflammation was observed. With short tangle fibers, inflammation was not observed. Accordingly, we anticipate that if longer fibers were used in our study, there would be more inflammation and more fibrosis. However, Muller et al. (2005) reported that ground MWCNTs (length 0.7 µm) produced more rapid inflammation and fibrosis than raw MWCNTs (length 5.9 µm) in intratracheal instillation study. Han et al. (2008) analyzed the geometric shapes of MWCNTs in experimental work environments in Korea where MWCNTs are handled, and found that the diameters of about 50 nm (personal exposure sample: 52 nm; working environment sample: 56 nm) and the tube length of about 1.5 µm (personal exposure sample: 1.47 µm; working environment sample: 1.76 µm) were the same sizes as the samples that we used in the present inhalation study. In the work environment, individual tubes, multiple tubes and tubular structures were also observed (Han et al. 2008; Johnson et al. 2010). Accordingly, the geometric shapes and dispersions of our samples may emulate those of the samples in the work environment.

Finally, we used dispersed MWCNTs to perform an inhalation study and an intratracheal instillation studies, and investigated the toxicity to the lungs. In the intratracheal instillation study, persistent lung inflammations and CINC-1 expressions were found at high doses; temporary inflammation was found at low doses. In the inhalation study, temporary and minimal pulmonary inflammation and temporary increase in CINC-1 to 3 expressions were found. From these results we conclude that MWCNTs have the potential to cause inflammation. These data in intratracheal instillation and inhalation studies suggest that well-dispersed MWCNTs have the potential of neutrophil inflammation.

Declaration of interest:

This research was funded by a grant from the New Energy and Industrial Technology Development Organization of Japan (NEDO) titled: "Evaluating risks associated with manufactured nanomaterials; Developing toxicity evaluating methods by inhalation exposure (P06041)". The authors report no conflicts of interest. The authors alone are responsible for the content and writing of the paper.

References

- Bide RW, Armour SJ, Yee R. 2000. Allometric respiration/body mass data for animals to be used for estimates of inhalation toxicity to young and adult humans. *J Appl Toxicol* 20:273-290.
- Borm PJA, Driscoll K. 1996. Particles, inflammation and respiratory tract carcinogenesis. *Toxicol Lett* 88(1):109-113.
- Card JW, Zeldin DC, Bonner JC, Nestmann ER. 2008. Pulmonary applications and toxicology of engineered nanoparticles. *Am J Physiol Lung Cell Mol Physiol* 295:L400-411.
- Darsono N, Yoon D-H, Kim J. 2008. Milling and dispersion of multi-walled carbon nanotubes in texanol. *Appl Sur Sci* 254:3412-3419.
- Dillon AC, Parilla PA, Alleman JL, Gennett T, Jones KM, Heben MJ. 2005. Systematic inclusion of defects in pure carbon single-wall nanotubes and their effect on the Raman D-band. *Chem Phys Lett* 401:522-528.
- Dresselhaus MS, Dresselhaus G, Saito R, Jorio A. 2005. Raman spectroscopy of carbon nanotubes. *Phys Rep* 409:47-99.
- Endo M. 1988. Grow carbon fibers in the vapor phase. *Chem Tech* 18:568-576.
- Fujita K, Morimoto Y, Ogami A, Tanaka I, Endoh S, Uchida K, Tao H, Akasaka M, Inada M, Yamamoto K, Fukui H, Hayakawa M, Horie M, Saito Y, Yoshida Y, Iwahashi H, Niki E, Nakanishi J. 2009. A gene expression profiling approach to study the influence of ultrafine particles on rat lungs. In: Kim JY, Platt U, Gu MB, Iwahashi H, editors. *Atmospheric and biological environmental monitoring*. Dordrecht: Springer Netherlands, pp. 219-227.
- Han JH, Lee EJ, So KP, Lee YH, Bae GN, Lee SB, Ji JH, Cho MH, Yu JJ. 2008. Monitoring multiwalled carbon nanotube in carbon nanotube research facility. *Inhal Toxicol* 20:741-749.
- Iijima S. 1991. Helical microtubes of graphitic carbon. *Nature* 354:56-58.
- Johnson DR, Methner MM, Kennedy AJ, Steevens JA. 2010. Potential for occupational exposure to engineered carbon-based nanomaterials in environmental laboratory studies. *Environ Health Perspect* 118:49-54.
- Kobayashi N, Naya M, Endoh S, Maru J, Yamamoto K, Nakanishi J. 2009. Comparative pulmonary toxicity study of nano-TiO₂ particles of different sizes and agglomerations in rats: Different short- and long-term post-instillation results. *Toxicology* 264:110-118.
- Kobayashi N, Naya M, Ema M, Endoh S, Maru J, Mizuno K, Nakanishi J. 2010. Biological response and morphological assessment of individually dispersed multi-wall carbon nanotubes in the lung after intratracheal instillation in rats. *Toxicology* 276:143-153.
- Kreyling WG, Semmler-Behnke M, Seitz J, Scymczak W, Wenk A, Mayer P, Takenaka S, Oberdörster G. 2009. Size dependence of the translocation of inhaled iridium and carbon nanoparticles aggregates from the lung of rats to the blood and secondary target organs. *Inhal Toxicol* 21(S1):55-60.
- Lam CW, James JT, McCluskey R, Hunter RL. 2004. Pulmonary toxicity of single-wall carbon nanotubes in mice 7 and 90 days after intratracheal instillation. *Toxicol Sci* 77:126-134.
- Lee S, Peng W Jr, Liu C-H. 2008. Raman study of carbon nanotube purification using atmospheric pressure plasma. *Carbon* 46:2124-2132.
- Liu S, Wei L, Hao L, Fang N, Chang M-W, Xu R, Yang Y, Chen Y. 2009. Sharper and faster "nano darts" kill more bacteria. A study of antibacterial activity of individually dispersed pristine single-walled carbon nanotube. *ACS Nano* 3:3891-3902.
- Ma-Hock L, Treumann S, Strauss V, Brill S, Luiz F, Mertler M, Wiench K, Gamer AO, van Ravenzwaay B, Landsiedel R. 2009. Inhalation toxicity of multi-wall carbon nanotubes in rats exposed for 3 months. *Toxicol Sci* 112:468-481.
- Mercer RR, Scabilloni J, Wang L, Kisin E, Murray AR, Schwegler-Berry D, Shvedova AA, Castranova V. 2008. Alteration of deposition pattern and pulmonary response as a result of improved dispersion of aspirated single walled carbon nanotubes in a mouse model. *Am J Physiol Lung Cell Mol Physiol* 294:87-97.
- Miller FJ. 2000. Dosimetry of particles in laboratory animals and humans in relationship to issues surrounding lung overload and human health risk assessment: A critical review. *Inhal Toxicol* 12:19-57.
- Mitchell LA, Gao J, Wal RV, Gigliotti A, Burchiel SW, McDonald JD. 2007. Pulmonary and systemic immune response to inhaled multiwalled carbon nanotubes. *Toxicol Sci* 100(1):203-214.
- Mitsuhashi H, Hata J, Asano S, Kishimoto T. 1999. Appearance of cytokine-induced neutrophil chemoattractant isoforms and immunolocalization of them in lipopolysaccharide-induced acute lung inflammation in rats. *Inflammation Res* 48:588-593.
- Morimoto Y, Kobayashi N, Shinohara N, Myojo T, Tanaka I, Nakanishi J. 2010a. Hazard assessments of manufactured nanomaterials. *J Occup Health* 52(6):325-334.

- Morimoto Y, Hirohashi M, Ogami A, Oyabu T, Myojo T, Nishi K, Kadoya C, Todoroki M, Yamamoto M, Murakami M, Shimada M, Wang WN, Yamamoto K, Fujita K, Endoh S, Uchida K, Shinohara N, Nakanishi J, Tanaka I. 2010b. Inflammogenic effect of well-characterized fullerenes in inhalation and intratracheal instillation studies. *Part Fibre Toxicol* 7:4.
- Morimoto Y, Ogami A, Todoroki M, Yamamoto M, Murakami M, Hirohashi M, Oyabu T, Myojo T, Nishi K, Kadoya C, Yamasaki S, Nagatomo H, Tanaka I, Fujita K, Endoh S, Uchida K, Yamamoto K, Kobayashi N, Nakanishi J. 2010c. Expression of inflammation-related cytokines following intratracheal instillation of nickel oxide nanoparticles. *Nanotoxicology* 4(2):161–176.
- Muller J, Huaux F, Moreau N, Misson P, Heilier JF, Delos M, Arras M, Fonseca A, Nagy JB, Lison D. 2005. Respiratory toxicity of multi-wall carbon nanotubes. *Toxicol Appl Pharmacol* 207:221–231.
- Muller J, Huaux F, Fonseca A, Nagy JB, Moreau N, Delos M, Raymundo-Piñero E, Béguin F, Kirsch-Volders M, Fenoglio I, Fubini B, Lison D. 2008a. Structural defects play a major role in the acute lung toxicity of multiwall carbon nanotubes: Physicochemical aspects. *Chem Res Toxicol* 21(9):1690–1697.
- Muller J, Huaux F, Fonseca A, Nagy JB, Moreau N, Delos M, Raymundo-Piñero E, Béguin F, Kirsch-Volders M, Fenoglio I, Fubini B, Lison D. 2008b. Structural defects play a major role in the acute lung toxicity of multiwall carbon nanotubes: Toxicological aspects. *Chem Res Toxicol* 21(9):1698–1705.
- Muller J, Delos M, Panin N, Rabolli V, Huaux F, Lison D. 2009. Absence of carcinogenic response to multiwall carbon nanotubes in a 2-year bioassay in the peritoneal cavity of the rat. *Toxicol Sci* 110:442–448.
- Musumeci AW, Wacławik ER, Frost RL. 2008. A comparative study of single-walled carbon nanotube purification techniques using Raman spectroscopy. *Spectrochim Acta Part A* 71:140–142.
- Mutlu GM, Budinger GR, Green AA, Urich D, Soberanes S, Chiarella SE, Alheid GF, McCrimmon DR, Szeleifer I, Hersam MC. 2010. Biocompatible nanoscale dispersion of single-walled carbon nanotubes minimizes in vivo pulmonary toxicity. *Nano Lett* 10(5):1664–1670.
- Nishi K, Morimoto Y, Ogami A, Murakami M, Myojo T, Oyabu T, Kadoya C, Yamamoto M, Todoroki M, Hirohashi M, Yamasaki S, Fujita K, Endo S, Uchida K, Nakanishi J and Tanaka I. 2009. Expression of cytokine-induced neutrophil chemoattractant in rat lungs by intratracheal instillation of nickel oxide nanoparticles. *Inhal Toxicol* 21(12):1030–1039.
- Oberdörster G, Oberdörster E, Oberdörster J. 2005. Nanotoxicology: An emerging discipline evolving from studies of ultrafine particles. *Environ Health Perspect* 113:823–839.
- Pacurari M, Yin XJ, Ding M, Leonard SS, Schwegler-Berry D, Ducatman BS, Chirila M, Endo M, Castranova V, Vallyathan V. 2008. Oxidative and molecular interactions of multi-wall carbon nanotubes (MWCNT) in normal and malignant human mesothelial cells. *Nanotoxicology* 2(3):155–170.
- Pauluhn J. 2010. Subchronic 13-week inhalation exposure of rats to multiwalled carbon nanotubes: Toxic effects are determined by density of agglomerate structures, not fibrillar structures. *Toxicol Sci* 113:226–242.
- Poland CA, Duffin R, Kinloch I, Maynard A, Wallace WAH, Seaton A, Stone V, Brown S, MacNee W, Donaldson K. 2008. Carbon nanotubes introduced into the abdominal cavity of mice show asbestos-like pathogenicity in a pilot study. *Nat Nanotechnol* 3:423–428.
- Rutishauser BR, Brown DM, Boyles MP, Kinloch IA, Windle AH, Gehr P, Stone V. 2010. Relating the physicochemical characteristics and dispersion of multiwalled carbon nanotubes in different suspension media to their oxidative reactivity in vitro and inflammation in vivo. *Nanotoxicology* 4(3):331–342.
- Sayes CM, Reed KL, Warheit DB. 2007. Assessing toxicity of fine and nanoparticles: Comparing in vitro measurements to in vivo pulmonary toxicity profiles. *Toxicol Sci* 97(1):163–180.
- Shacter E, Weitzman SA. 2002. Chronic inflammation and cancer. *Oncology* 16:217–232.
- Shvedova AA, Kisin ER, Mercer R, Murray AR, Johnson VJ, Potapovich AI, Tyurina YY, Gorelik O, Arepalli S, Schwegler-Berry D, Hubbs AF, Antonini J, Evans DE, Ku BK, Ramsey D, Maynard A, Kagan VE, Castranova V, Baron P. 2005. Unusual inflammatory and fibrogenic pulmonary responses to single-walled carbon nanotubes in mice. *Am J Physiol Lung Cell Mol Physiol* 289(5):L696–708.
- Vankoningsloo S, Piret JP, Saout C, Noel F, Mejia J, Zouboulis CC, Delhalle J, Lucas S, Tousaint O. 2010. Cytotoxicity of multi-walled carbon nanotubes in three skin cellular models: Effects of sonication, dispersive agents and corneous layer of reconstructed epidermis. *Nanotoxicology* 4(1):84–97.
- Wang L, Castranova V, Mishra A, Chen B, Mercer RR, Schwegler-Berry D, Rojanasakul Y. 2010. Dispersion of single-walled carbon nanotubes by a natural lung surfactant for pulmonary in vitro and in vivo studies. *Part Fibre Toxicol* 7:31.
- Warheit DB, Laurence BR, Reed KL, Roach DH, Webb TR. 2004. Comparative pulmonary toxicity assessment of single-wall carbon nanotubes in rats. *Toxicol Sci* 77:117–125.
- Wepasnick KA, Smith BA, Bitter JL, Fairbrother DH. 2010. Chemical and structural characterization of carbon nanotube surfaces. *Anal Bioanal Chem* 396:1003–1014.
- Yokota S, Seki T, Furuya M, O'Hara N. 2005. Acute functional enhancement of circulatory neutrophils after intratracheal instillation with diesel exhaust particles in rats. *Inhal Toxicol* 17(12):671–679.